Multiturn extraction and injection by means of adiabatic capture in stable islands of phase space

R. Cappi and M. Giovannozzi
CERN, CH 1211 Geneva 23, Switzerland
(Received 10 September 2003; published 5 February 2004)

Recently a novel approach has been proposed for performing multiturn extraction from a circular machine. Such a technique consists of splitting the beam by means of stable islands created in transverse phase space by magnetic elements creating nonlinear fields, such as sextupoles and octupoles. Provided a slow time variation of the linear tune is applied, adiabatic with respect to the betatron motion, the islands can be moved in phase space and eventually charged particles may be trapped inside the stable structures. This generates a certain number of well-separated beamlets. Originally, this principle was successfully tested using a fourth-order resonance. In this paper the approach is generalized by considering other types of resonances as well as the possibility of performing multiple multiturn extractions. The results of numerical simulations are presented and described in detail. Of course, by time reversal, the proposed approach could be used also for multiturn injection.

DOI: 10.1103/PhysRevSTAB.7.024001 PACS numbers: 29.27.Ac, 29.27.Bd, 05.45.–a

I. INTRODUCTION

A special technique is normally used to fill the CERN Super Proton Synchrotron (SPS) with a high-intensity proton beam delivered by the proton synchrotron (PS), the so-called continuous transfer (CT) [1]. The beam is sliced using an electrostatic septum: by properly defining a closed orbit perturbation and by setting the horizontal tune equal to $Q_H = 6.25$ the beam is extracted from the PS over five consecutive turns. A continuous ribbon four-turn long is extracted first, while the remaining central core is extracted last thus generating a proton spill five-turn long (see Refs. [1,2] for more details). Such a multiturn extraction might not be the best choice for the planned CERN Neutrino to Gran Sasso proton beam [3], especially in case of an intensity upgrade [4], due to the intrinsic losses, of the order of 15%–20% of the overall proton intensity onto the electrostatic septum as well as the poor betatron matching of the resulting slices. Detailed analytical computations of the expected betatron mismatch and potential emittance blowup at injection into the SPS have been reported in Ref. [2].

An alternative method was proposed [5,6]. The beam is split in the transverse horizontal phase space by trapping particles inside stable islands created by sextupole and octupole magnets. The tune has to be varied in order to create the appropriate phase space topology [5]. The principle consists of sweeping through the chosen resonance to change the phase space topology from a situation where no islands are present, to a final stage where stable islands are created. During the resonance crossing stage, small islands appear around the origin of phase space occupied by the beam. Therefore, particles can get trapped inside the stable structures, thus generating a number of beamlets proportional to the resonance order. Such beamlets are eventually transported towards higher amplitudes by changing the tune to increase their separation and to produce regions emptied of particles in between the beamlets [5]. At this stage, it is possible to induce a distortion of the beam closed orbit to jump a septum, whose blade will be located in the empty space between the beamlets. Therefore, the beam is extracted over many turns without the need of any intercepting device to split it, thus reducing the losses. In addition, as shown in Ref. [2], the betatron mismatch is greatly improved with respect to, e.g., the present CT extraction. It is important to stress that this approach is not affected by particle detrapping, typical of modulational diffusion (see Ref. [7] for a general overview of the problem) as the tune variation is not periodic.

For the specific CERN application the fourth-order resonance was studied [5]. However, following the encouraging results, numerical simulations were performed also for the third-order resonance [6] showing the validity of the method in that case.

Preliminary experimental results obtained during the 2002 run of the PS machine allowed observing the trapping process into stable islands of phase space in real machines [8]. In this paper the latest results of numerical simulations are presented, showing how to perform multiturn extraction over a small number of turns, from two to six, using adiabatic trapping inside a properly chosen resonance. Other possibilities are also explored, such as the option of performing multiple multiturn extractions.

The longitudinal structure of a beam extracted over a few turns deserves a few comments. In the present CT, the beam is debunched, to cancel the 10 MHz structure, and then partially recaptured using 200 MHz cavities just prior to the slicing process. Therefore, the extracted ribbon features a longitudinal modulation on top of the continuous structure. As far as the novel approach is concerned, both bunched and unbunched beams can be split by means of trapping inside stable islands, the only issue being the tune modulation induced by the longitudinal dynamics, which might generate emittance blowup of the beamlets.

The plan of this paper is the following: in Sec. II the model used in the numerical simulations is presented and discussed, while in Sec. III the results of the numerical simulations for various resonances, ranging from second order (Sec. III A) to fifth order (Sec. III D), are presented, with particular emphasis for the fourth-order resonance (Sec. III C) in view of its potential applications to the CERN PS machine. In Sec. IV results concerning multiple multiturn extraction are presented and some conclusions are drawn in Sec. V. Finally, two appendices report in detail the way the one-turn transfer map is computed (Appendix A) and some results concerning fixed points of symplectic maps (Appendix B) relevant for the model used for the two-turn extraction.

II. NUMERICAL MODEL

The computation of the one-turn transfer map depends on the assumption made for the structure of the circular machine under study. By assuming that the magnets generating the nonlinear magnetic fields are located at the same place in the ring, and that the effect on the beam dynamics is represented using the single-kick approximation [9], then the one-turn transfer map is a Hénon-like [10] 4D polynomial map, which can be expressed as $\hat{\mathbf{X}}_{n+1} = \mathbf{M}_n(\hat{\mathbf{X}}_n)$:

$$\begin{pmatrix} \hat{X} \\ \hat{X}' \\ \hat{Y} \\ \hat{Y}' \end{pmatrix}_{n+1} = R(\omega_x, \omega_y) \begin{pmatrix} \hat{X} \\ \hat{X}' + \hat{X}^2 - \chi\hat{Y}^2 + \kappa(\hat{X}^3 - 3\chi\hat{X}\hat{Y}^2) \\ \hat{Y} \\ \hat{Y}' + -2\chi\hat{X}\,\hat{Y} - \kappa(\chi^2\hat{Y}^3 - 3\chi\hat{X}^2\hat{Y}) \end{pmatrix}_n . \tag{1}$$

The components of the vector $(\hat{X}, \hat{X}', \hat{Y}, \hat{Y}')$ are dimensionless coordinates allowing us to set the coefficient of the quadratic term of the map (1) to one. More details on the relations between physical, Courant-Snyder [11], and coordinates used here can be found in Appendix A.

The manipulations required to capture the beam inside stable islands are performed in the horizontal plane only. This means that, provided the vertical tune is chosen carefully as to avoid low-order resonances, the vertical degree of freedom can be safely neglected in the numerical simulations and the map (1) can be replaced by the 2D one-turn map given by

$$\begin{pmatrix} \hat{X} \\ \hat{X}' \end{pmatrix}_{n+1} = R(\omega_x) \begin{pmatrix} \hat{X} \\ \hat{X}' + \hat{X}^2 + \kappa\hat{X}^3 \end{pmatrix}_n . \tag{2}$$

This approach is used for most of the multiturn extraction schemes presented in this paper, unless for the special case of the five-turn extraction, where 4D simulations have been performed and they confirm that the neglected vertical degree of freedom does not alter the result obtained with the 2D map (2).

The case of two-turn extraction deserves special consideration. In fact, 2D one-turn transfer maps of the form (2) do not have any fixed point of the order of 2. This is a consequence of the symmetry induced by locating the sextupole and octupole in the same section of the machine (the reason for this is discussed in detail in Appendix B). If this condition is broken, one can find a class of maps with fixed points, and stable islands, of period two. This is the case of the following maps:

$$\begin{pmatrix} \hat{X} \\ \hat{X}' \end{pmatrix}_{n+1} = R(\omega_x) \circ \mathcal{K}_{\text{sextupole}} \circ R(\bar{\omega}) \circ \mathcal{K}_{\text{octupole}}(\hat{X}, \hat{X}')_n . \tag{3}$$

The polynomial maps $\mathcal{K}_{\text{sextupole}}, \mathcal{K}_{\text{octupole}}$ represent sextupolar and octupolar kicks, respectively, of the form

$$\mathcal{K}_{\text{sextupole}}(\hat{X}, \hat{X}') = \begin{pmatrix} \hat{X} \\ \hat{X}' + \hat{X}^2 \end{pmatrix},$$
$$\mathcal{K}_{\text{octupole}}(\hat{X}, \hat{X}') = \begin{pmatrix} \hat{X} \\ \hat{X}' + \kappa\hat{X}^3 \end{pmatrix}. \tag{4}$$

In the numerical simulations presented in this paper $\bar{\omega} = \pi/2$ and ω_x is chosen so that $\omega_x + \bar{\omega}$ has the correct value, i.e., near the half-integer resonance.

The other key ingredient for the novel extraction, in combination with the stable islands, is the tune variation. In the model used for the numerical simulations the horizontal tune is changed in the following way:

$$\omega_x(n) = \begin{cases} \omega_{x,a} + (\omega_{x,b} - \omega_{x,a})(\frac{n-1}{n_1-1})^p & \text{if } n \le n_1, \\ \omega_{x,b} & \text{if } n_1 < n \le n_2, \\ \omega_{x,b} + (\omega_{x,c} - \omega_{x,b})(\frac{n-n_2}{n_3-n_2}) & \text{if } n_2 < n \le n_3, \end{cases} \tag{5}$$

where $\omega_{x,a}$, $\omega_{x,b}$, and $\omega_{x,c}$ are the initial, intermediate, and final tune values, respectively; n_1, n_2, and n_3 represent the turn number of transition between the stage of resonance crossing and constant tune, constant tune and linear ramp to separate islands before extraction, and the time when extraction is ready to occur, respectively. Finally, p is a parameter used to change the functional dependence of the tune variation on n during the resonance crossing: it allows changing from a linear sweep to a power law, thus changing the speed of resonance crossing. All these parameters have not yet been fully optimized, and this point is the subject of further studies. The vertical tune is always kept constant in 4D simulations.

III. RESULTS OF NUMERICAL SIMULATIONS

The polynomial map (1) or the two-dimensional versions (2) and (3) have been used to study the trapping

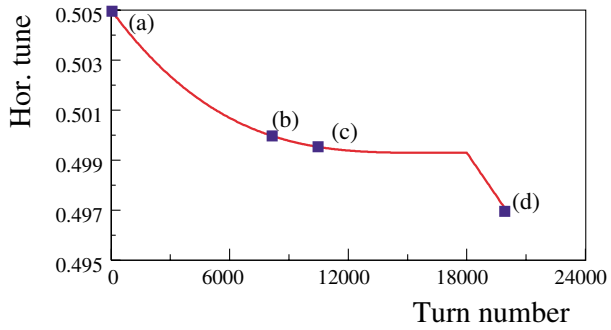

FIG. 1. (Color) Evolution of the tune used for the simulation of a two-turn extraction ($p = 3$). The four points labeled with letters correspond to the tune values at which the beam distribution is shown in Fig. 2.

process, with particular emphasis on losses during such a manipulation as these are the only losses possible for the proposed extraction scheme. In fact, having removed any particle from the region in between the stable islands, the extraction septum cannot intercept any beam particle.

A. Two-turn extraction

Starting from the lowest-order resonance, it is possible to use the half-integer resonance as the base for a two-turn extraction. In Fig. 1 the tune as a function of turn number is shown. The four points labeled with letters refer to the tune values at which the beam distribution is shown in Fig. 2. The computations are performed using the map (3).

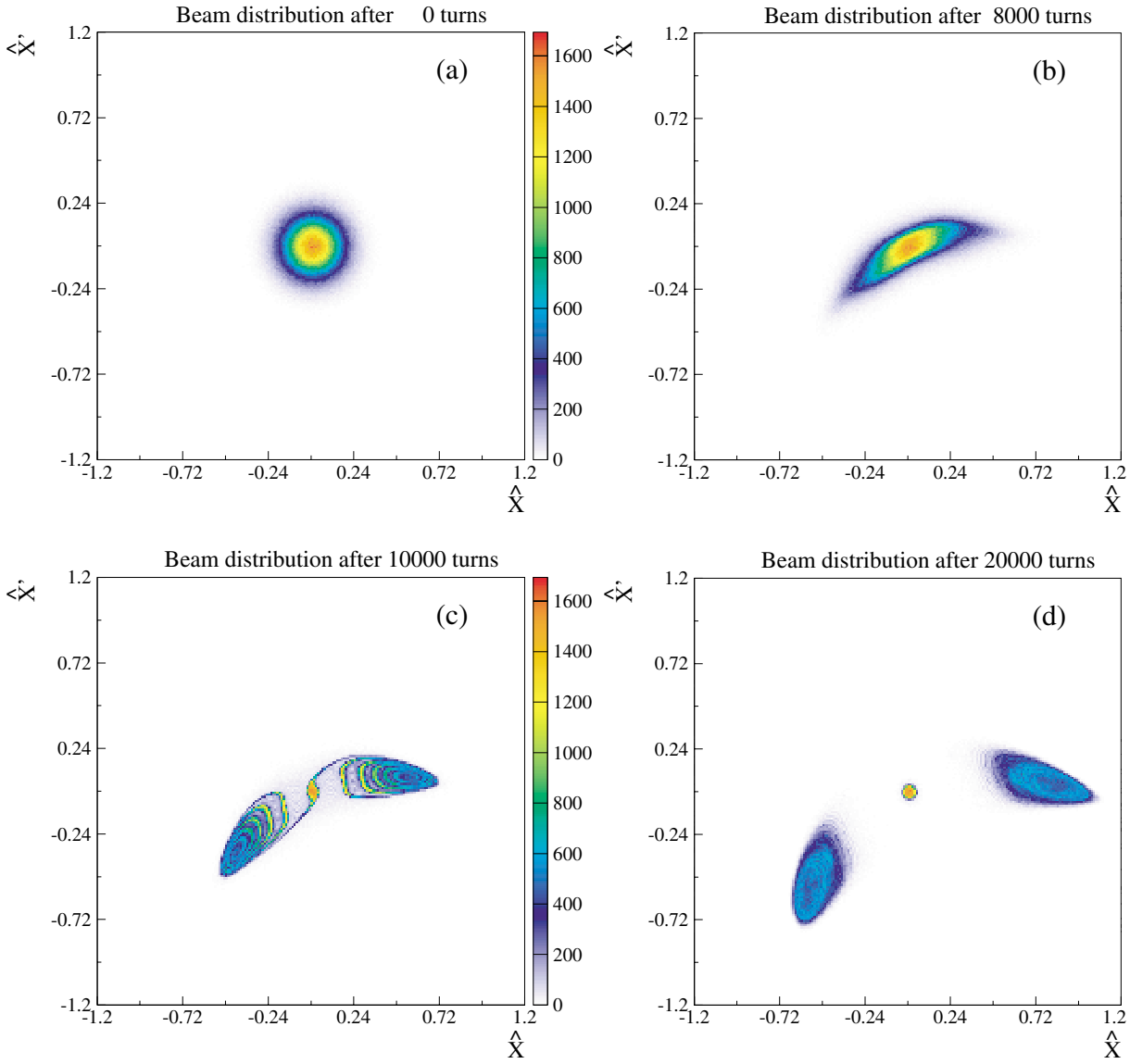

FIG. 2. (Color) Beam distribution during the trapping process with two islands (8.1×10^5 initial conditions). The initial distribution is a Gaussian centered on zero, with a standard deviation $\sigma = 0.11$, $\kappa = -1$. Only a few particles are left near the origin of phase space.

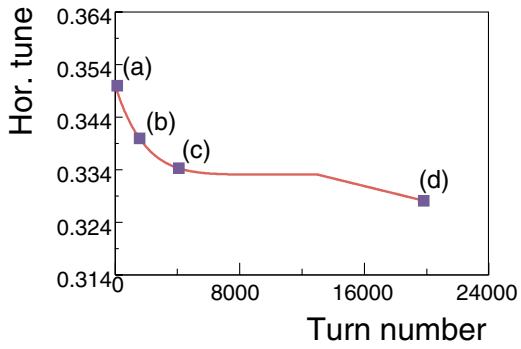

FIG. 3. (Color) Evolution of the tune used for the simulation of a three-turn extraction ($p = 7$). The four points labeled with letters correspond to the tune values at which the beam distribution is shown in Fig. 4.

The adiabatic capture inside the two stable islands is clearly visible. As the stable phase space region around the origin shrinks when approaching the resonance, particles are repelled from the origin during the trapping stage. Therefore, only a small fraction of particles remains near the origin, while the majority of them migrates to the islands as the tune is swept through the half-integer resonance. Once the two beamlets are created, it is possible to move the islands towards higher amplitudes, hence increasing the beamlets separation to prepare for extraction.

B. Three-turn extraction

In this case the model (2) is used in the numerical simulations. The time evolution of the linear tune is presented in Fig. 3, while the evolution of the beam distribution is shown in Fig. 4.

Also in this case the resonance is unstable, i.e., the stable region around the origin shrinks when approaching the resonance, thus making it possible to deplete almost perfectly the region near the origin of phase space. Three beamlets represent the final result of the capture process.

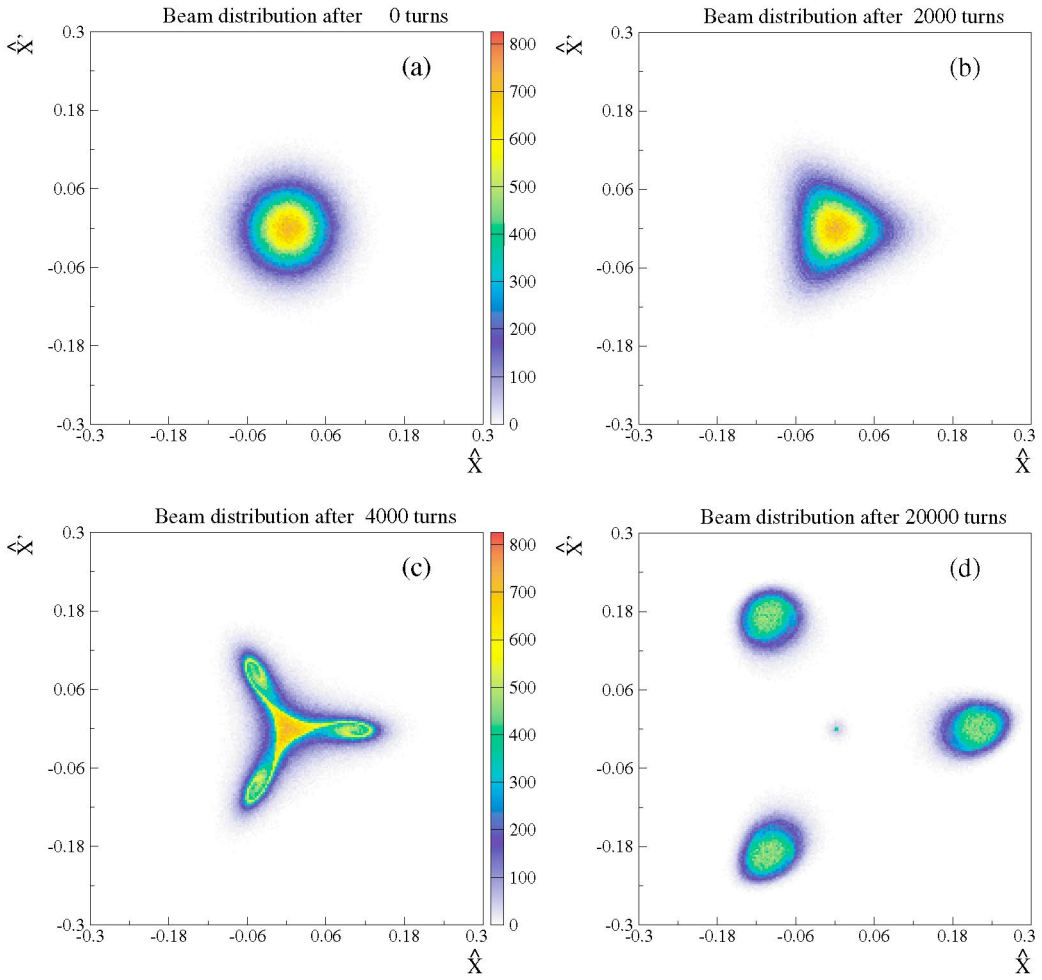

FIG. 4. (Color) Beam distribution during the trapping process with three islands (8.1×10^5 initial conditions). The initial distribution is a Gaussian centered on zero, with standard deviation $\sigma = 0.04$, $\kappa = -5$. Even in this case very few particles are left in the central part of phase space.

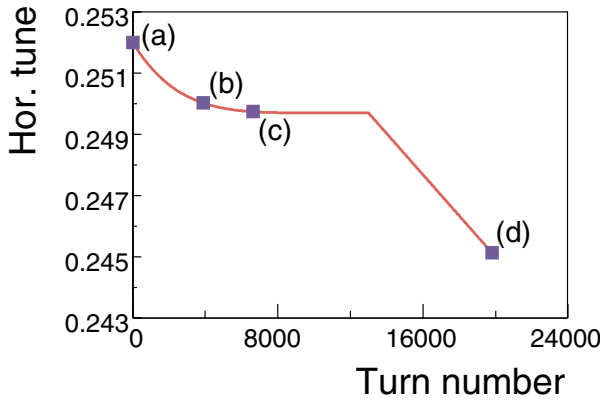

FIG. 5. (Color) Evolution of the tune used for the simulation of a five-turn extraction ($p = 5$). The four points labeled with letters correspond to the tune values at which the beam distribution is shown in Fig. 6.

C. Five-turn extraction

The fourth-order resonance is the one used in the original proposal [5] for a novel multiturn extraction to replace the present CT extraction mode. As the fourth-order resonance is stable for the system (2), the beam will be split into five beamlets. The evolution of the tune is shown in Fig. 5.

The evolution of the beam distribution is plotted in Fig. 6. The four outermost beamlets are created by adiabatic trapping inside the stable islands, while the fifth one is generated by those particles left unperturbed near the origin of phase space. This fact has deep implications on the properties of the beamlets. In fact, for the previous multiturn extraction processes (two and three turn) the various beamlets had exactly the same number of particles trapped inside as they represent a unique ribbon of length 2 or 3 times the machine circumference. On the

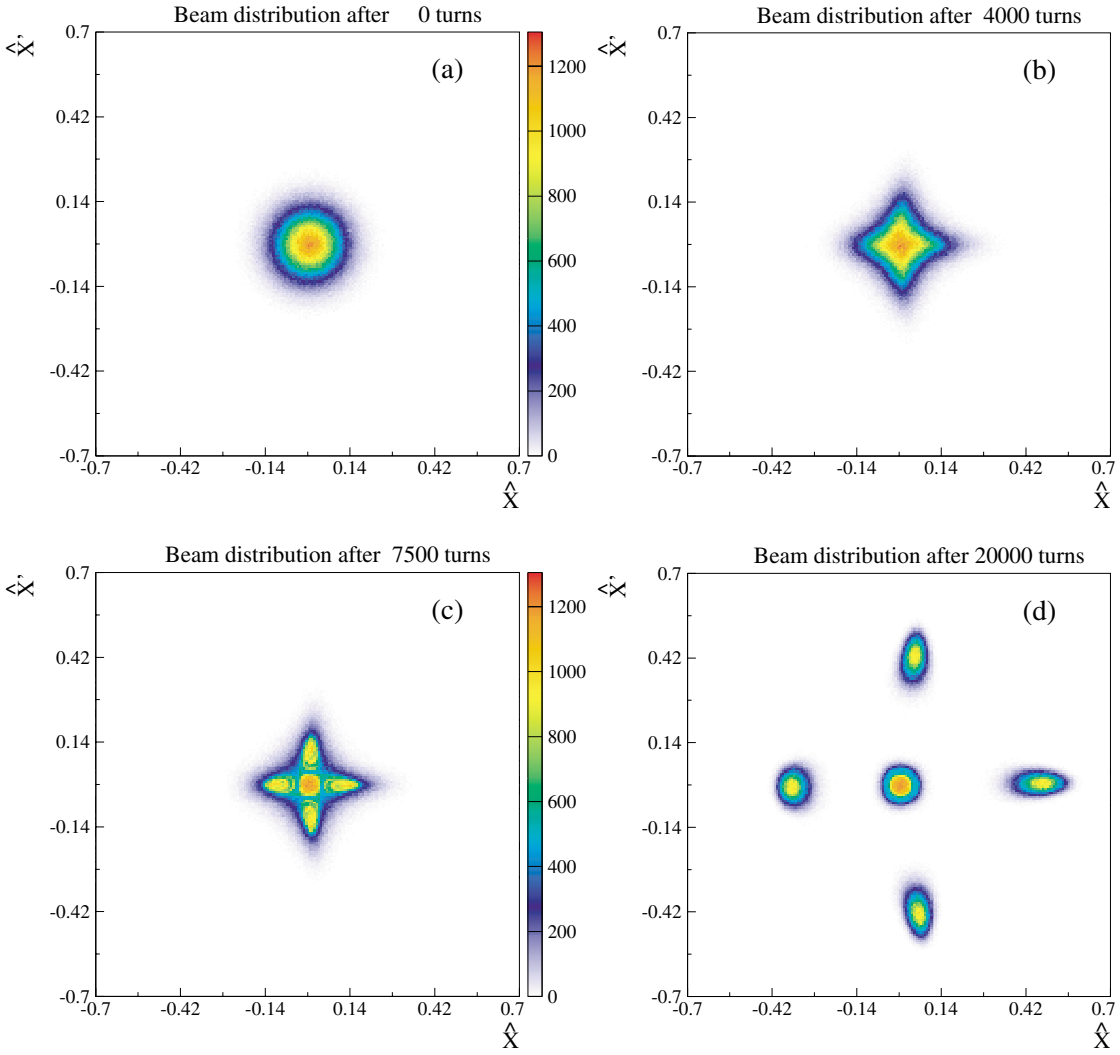

FIG. 6. (Color) Beam distribution during the trapping process with four islands (8.1×10^5 initial conditions). The initial distribution is a Gaussian centered on zero, with standard deviation $\sigma = 0.073$, $\kappa = -1.5$.

other hand, whenever the central part of phase space remains filled at the end of the capture process, it is not necessarily equally populated as the other beamlets, unless a dedicated optimization of the free parameters is performed. Such an optimization concerns mainly the sigma of the initial beam distribution, the nonlinear elements strength, and the properties of the tune variation.

For this specific case, 4D simulations have been performed using the map (1). The results are shown in Fig. 7, where two projections of the 4D phase space, namely, the physical phase space $(\hat{X}, \hat{Y})$ (left panel) and the vertical phase space $(\hat{Y}, \hat{Y}')$ (right panel) are shown.

In the physical phase space three spots are clearly shown, as a result of projecting the two beamlets centered on $\hat{X}' \neq 0$ onto the central one. The separation of the three spots can be adjusted by acting on the value of the final tune $\omega_{x,c}$. In the vertical phase space almost no sign of coupling with the horizontal one, due to the nonlinear terms in the map (1), is visible. This confirms that the assumption of neglecting this degree of freedom is well justified.

Another test performed for this special case was the sensitivity of the capture process on the presence of tune modulation. This is an almost unavoidable effect in real machines. It is potentially harmful for the proposed multiturn extraction because islands are shaken due to the periodic tune variation, thus inducing beam filamentation and emittance growth. Numerical simulations have been carried out including a tune ripple of the form

$$\hat{\omega}_x(n) = \omega_x(n)[1 + a\cos(2\pi f_{\text{ripple}} T_{\text{rev}} n)], \qquad (6)$$

where $\omega_x(n)$ is the function (5). The parameters a, f_{ripple}, the ripple amplitude and frequency in Hertz, respectively, have realistic values for the CERN PS machine, i.e., a about 10^{-3} and f_{ripple} in the range 50–600 Hz. T_{rev} is the revolution time, which is about 2.2 μs for the PS machine at 14 GeV/c. The results are shown in Fig. 8.

They confirm that the ripple is potentially harmful for the proposed extraction based on adiabatic capture. In fact, in all the cases shown in Fig. 8 the central beamlet is almost unaffected, while the four outermost beamlets show signs of degradation (emittance growth), visible in the form of an extended halo of particles surrounding the beamlets core. Of course, before concluding on the quantitative effect of the tune ripple on the extracted beam parameters, a more realistic model of the accelerator for which the extraction is designed has to be used in the numerical simulations.

D. Six-turn extraction

It is possible to further increase the length of the extracted spill by using even higher-order resonances. Here, the case of a resonance of order 5 is shown in Figs. 9 and 10. However, it is clear that there are intrinsic limitations on the resonance order. In fact, the higher the order, the smaller the islands' size, thus enhancing the difference between the first turns and the last one, represented by the particles left around the origin in phase space at the end of the capture process. Furthermore, it will be more and more difficult to create enough free space between the beamlets to accommodate the blade of an extraction septum.

IV. DIGRESSION: MULTIPLE MULTITURN EXTRACTION

From the results presented in the previous sections, it is clear that the number of extracted turns depends on the resonance order r and also on its stability. In fact, if the resonance is stable then the number of turns is equal to $r + 1$, otherwise it is simply r. As far as the extraction is

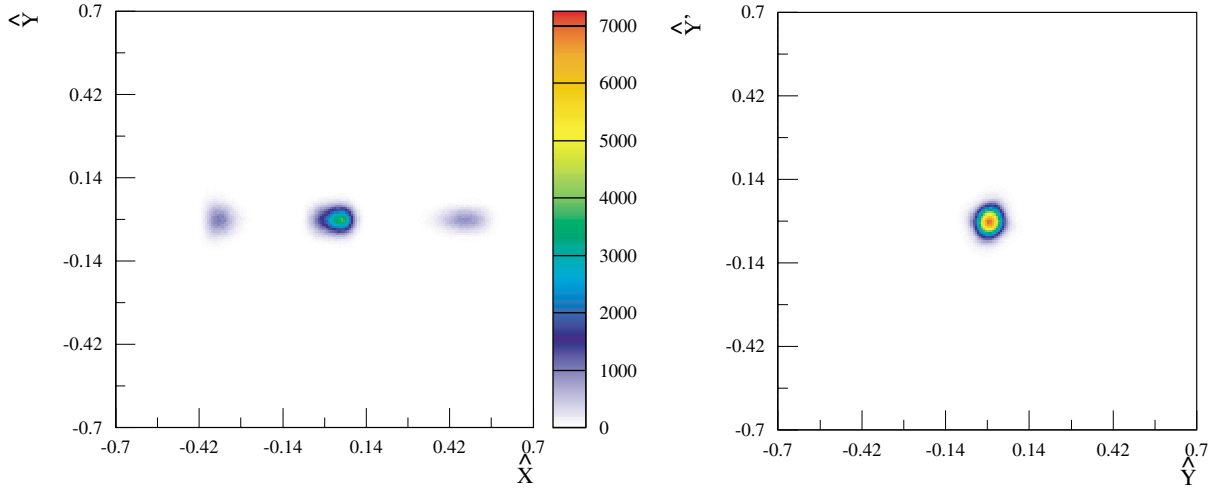

FIG. 7. (Color) Phase space projections: physical space $(\hat{X}, \hat{Y})$ (left panel) and vertical phase space $(\hat{Y}, \hat{Y}')$ (right panel) of the capture process with four islands as computed using the 4D map (1) with $\kappa = -1.5$ and $\chi = 0.5$. The vertical tune ν_y is 0.29.

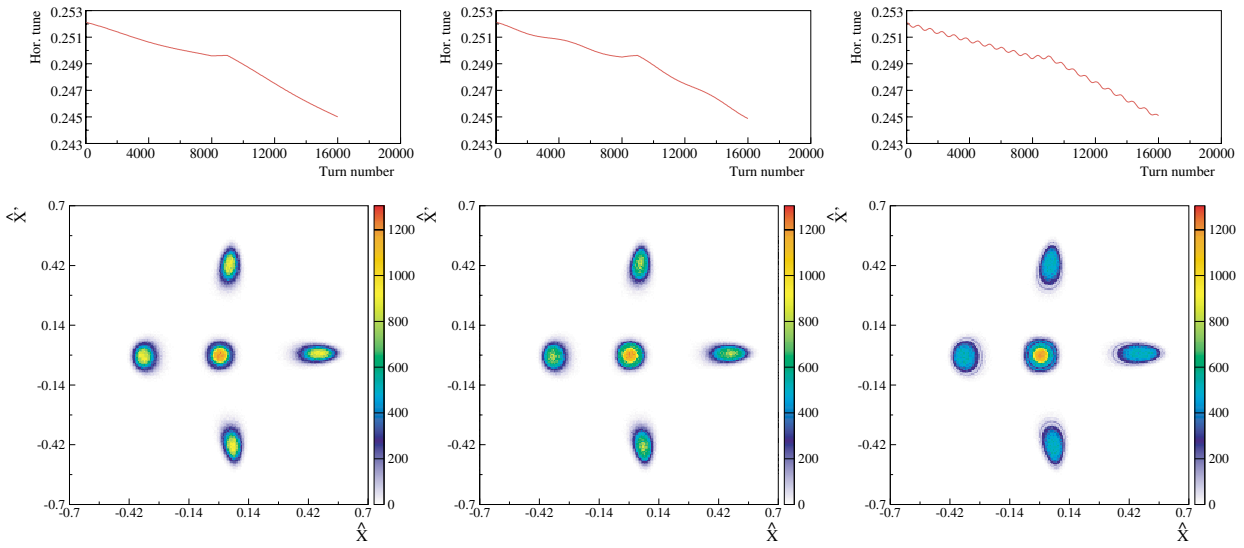

FIG. 8. (Color) Dependence on the tune ripple of beam distribution at the end of the capture process, i.e., after 2×10^4 turns (8.1×10^5 initial conditions) for different values of the ripple frequency. The initial distribution is a Gaussian centered on zero, with standard deviation $\sigma = 0.073$. The ripple parameters are $a = 10^{-3}$, and $b = 50$ Hz (left panel), 100 Hz (center panel), and 600 Hz (right panel). In this case $p = 1$.

concerned, it would be somewhat more difficult for the case of stable resonances, as the amplitude of the orbit distortion needed to extract the various beamlets would be different, i.e., the same for the first r turns, but larger for the last turn. This point could be difficult to solve. Therefore, in this section alternative solutions are proposed, based on the idea that the adiabatic capture can be repeated by splitting the central beamlet remaining from the previous extraction.

As an example, a possible scenario is presented in Fig. 11. The key parameters, such as the number of particles, the value of the parameter κ, and the horizontal tune, are plotted as a function of the turn number n.

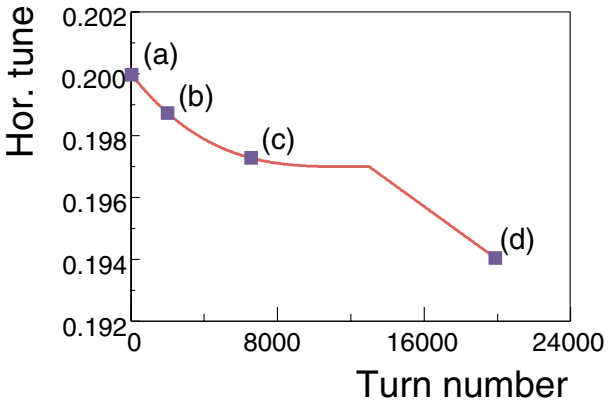

FIG. 9. (Color) Evolution of the tune used for the simulation of a six-turn extraction ($p = 3$). The four points labeled with letters correspond to the tune values at which the beam distribution is shown in Fig. 10.

The tune is periodically swept through the chosen resonance, in this case the fourth order, to periodically capture particles from the central beamlet. However, a problem appears, as the emittance of the beam core shrinks after each capture, due to the transfer and extraction of particles. To overcome this difficulty, two techniques can be used, namely, (i) change the parameter κ or (ii) increase artificially the beam emittance of the remaining beam core.

The first approach is shown in Fig. 11, where κ is increased. This is necessary as the islands' size is proportional to κ and it increases with the value of the tune. Just after crossing the resonant value, tiny islands are created near the origin: their size increases, as well as their separation, by moving the tune far apart from the resonance. As the central beamlet shrinks in size after successive multiturn extractions, particles will experience the influence of smaller and smaller islands. Therefore, to capture enough beam it is necessary to increase the islands' size by acting on the value of κ. The results of numerical simulations based on this principle are shown in Fig. 12. The letters refer to the corresponding tune value in Fig. 11.

The different stages are clearly visible as well as the effect of size reduction of the central beamlet. The approach seems to work well, no particle is lost in the simulations, and the various beamlets are always well separated without particles in between. Of course, a possible drawback could be the increasing strength of the sextupole and octupole, i.e., κ, required to capture the beam in the successive multiturn extractions.

The second approach, however, avoids increasing κ, as an appropriate emittance blowup is applied to the central

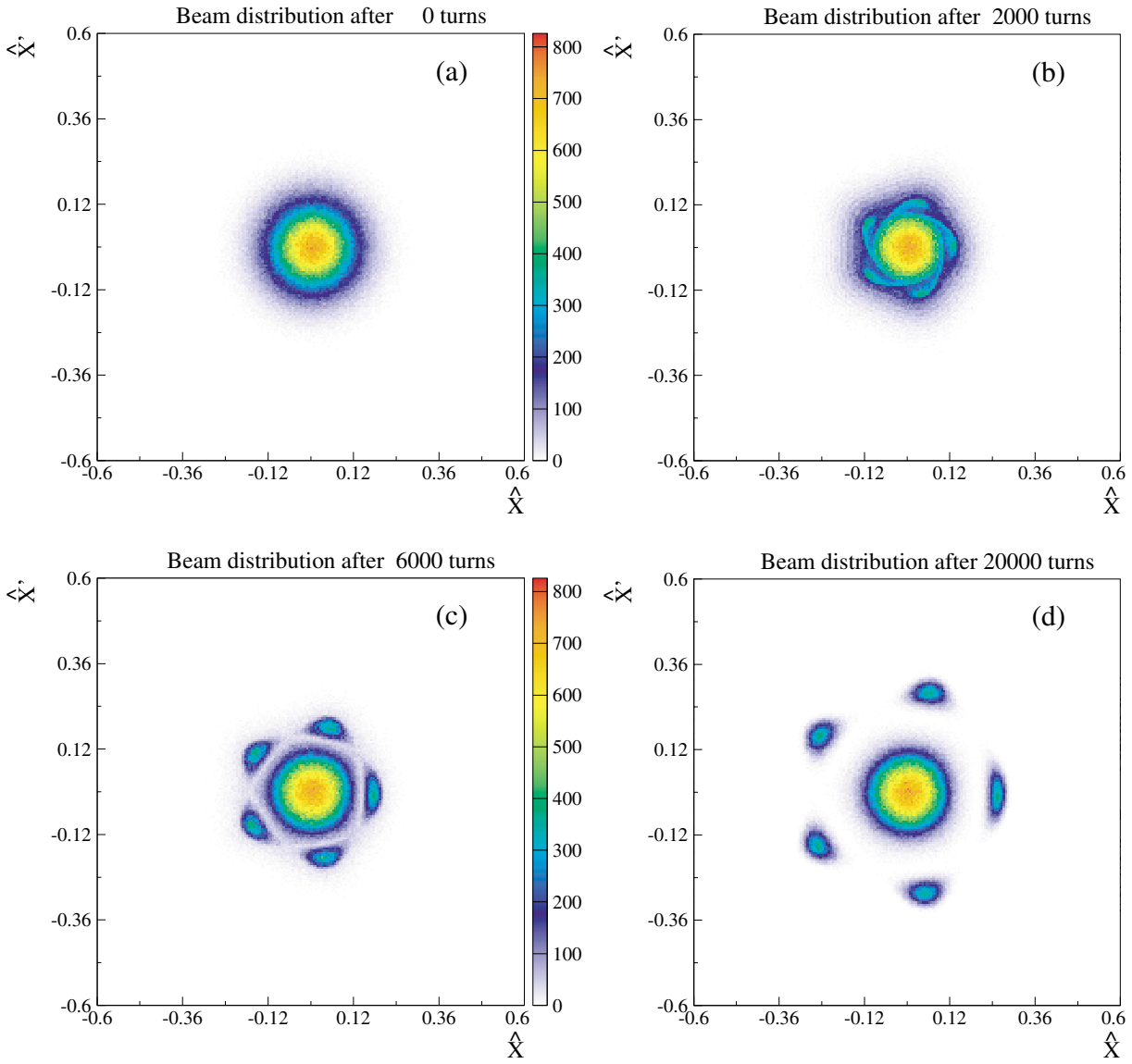

FIG. 10. (Color) Beam distribution during the trapping process with five islands (8.1×10^5 initial conditions). The initial distribution is a Gaussian centered on zero, with standard deviation $\sigma = 0.08$, $\kappa = -2$.

beamlet to keep its size almost constant, even after successive multiturn extractions. This is achieved by repeatedly kicking the beamlet when the tune is constant and back to its initial value, i.e., between stage (d) and (e) in Fig. 11. The results of numerical simulations are shown in Fig. 13.

Even this approach seems to work well, without beam losses during the capture process. The effect of the kicks used to blow up the beam is clearly visible. The main advantage with respect to the previous solution is that in this case the nonlinear effects are not enhanced after each extraction.

Finally, we would like to add that other approaches could be applied to extract the central beamlet left as a result of an adiabatic capture performed with a stable resonance. Those previously described would allow a periodic sequence of multiturn extractions. However, one could think of combining a particle trapping using a stable resonance, followed by an adiabatic capture performed using an unstable resonance. In this way, the whole beam would be extracted by means of only two steps.

V. CONCLUSIONS

In this paper various schemes for multiturn extraction based on adiabatic capture of charged particles in stable islands of phase space were presented. By choosing the appropriate resonance, two-, three-, five-, and six-turn extractions have been computed. In all the cases shown here, particles can be trapped inside islands without any loss. Furthermore, it is possible to move the beamlets by

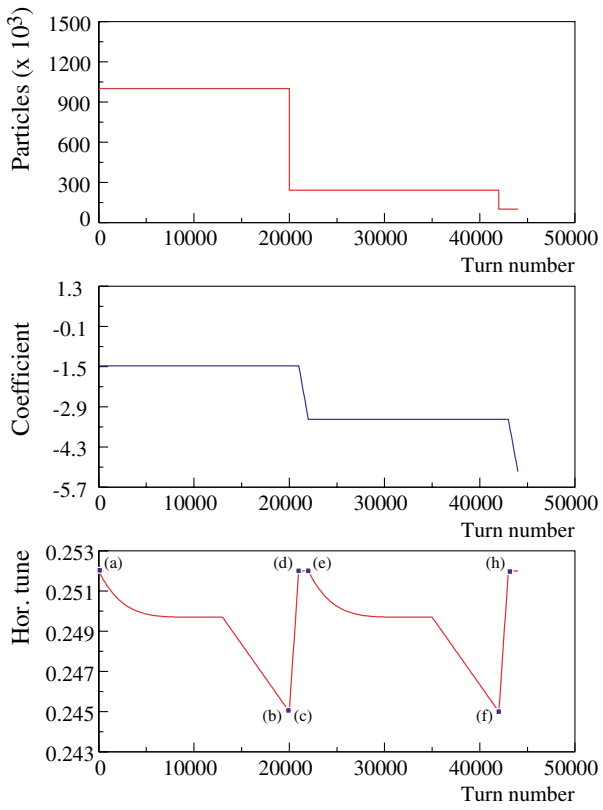

FIG. 11. (Color) Evolution of the main parameters during the multiple multiturn extraction: number of particles (top panel), κ (center panel), and horizontal tune (bottom panel). The points labeled with letters correspond to the tune values at which the beam distribution is shown in the subsequent Figs. 12 and 13. In this case $p = 5$.

acting on the tune to increase their separation, which is the necessary condition to allow the actual beam extraction to take place. For the case of the five-turn extraction, detailed analysis including 4D simulations and the study of the influence of tune ripple on the beam parameters at the end of the capture process were performed. 4D simulations confirm that the neglected degree of freedom does not affect the final result much, provided the vertical tune is chosen far away from low-order resonances. Tune ripple is known to be potentially harmful as it tends to move islands and, during the capture process, this might lead to emittance growth of the beamlets. However, at least for the case of the ripple parameters used in this study, which represent reasonable values for the CERN PS machine, the net effect is acceptable. In the case of stable resonances, multiple multiturn extractions are possible to repeatedly split the beam core left over previous extractions. Two approaches have been presented, combining the necessary tune variation to sweep periodically through the chosen resonance, together with either an increase of κ (to compensate for the shrinking of the beam core) or repeated kicks used to blow up the beam core. Both techniques seem to work well.

Last but not least, it is important to stress that the novel approach presented here, and applied to various types of multiturn extractions, can be used also in the case of multiturn injection by simply exploiting the symmetry under time reversal of the models used in the numerical simulations presented in this paper.

Further studies are in progress to quantify a number of issues such as the condition for the capture process to be adiabatic, the optimization of the tune variation, and the dependence of the extracted beam parameters on the strength of sextupole and octupole magnets.[1]

APPENDIX A: ONE-TURN TRANSFER MAPS

The 4D one-turn transfer map of a circular machine including localized sources of nonlinearities can be written as

$$\begin{pmatrix} x \\ x' \\ y \\ y' \end{pmatrix}_{n+1} = M \begin{pmatrix} x \\ x' + f_x(x, y) \\ y \\ y' + f_y(x, y) \end{pmatrix}_n, \tag{A1}$$

where (x, x', y, y') is a vector in the 4D phase space representing the particle's coordinates at the entrance of the magnetic elements generating nonlinear fields. M is a 4×4 matrix in block diagonal form, namely,

$$M = \begin{pmatrix} M_x & 0 \\ 0 & M_y \end{pmatrix}, \tag{A2}$$

with $M_{x,y}$ being 2×2 matrices. This form is certainly valid in case no sources of linear coupling, such as skew quadrupoles or solenoids, are present in the machine. Otherwise, it is always possible to decouple the linear matrix by using the formalism presented in Ref. [12].

The functions f_x, f_y are related to the nonlinearities in the machine. By using the single-kick approximation, it is possible to show that [9]

$$\begin{aligned} f_x(x, y) &= \Re \sum_{n=2}^{m} \frac{K_n + iJ_n}{n!}(x + iy)^n, \\ f_y(x, y) &= \Im \sum_{n=2}^{m} \frac{K_n + iJ_n}{n!}(x + iy)^n, \end{aligned} \tag{A3}$$

where the coefficients K_n, J_n, respectively, the normal and skew normalized integrated multipole strengths, are defined by

$$K_n = \frac{1}{B_0\rho}\frac{\partial^n B_y}{\partial x^n}\ell, \qquad J_n = \frac{1}{B_0\rho}\frac{\partial^n B_x}{\partial x^n}\ell, \tag{A4}$$

with m is the order of the highest multipole considered.

In Eq. (A4), $B_0\rho$ stands for the magnetic rigidity of the reference particle, B_x, B_y are the transverse components

[1] In a completely different context, the analysis of particle trapping through nonlinear resonance was discussed in Ref. [16].

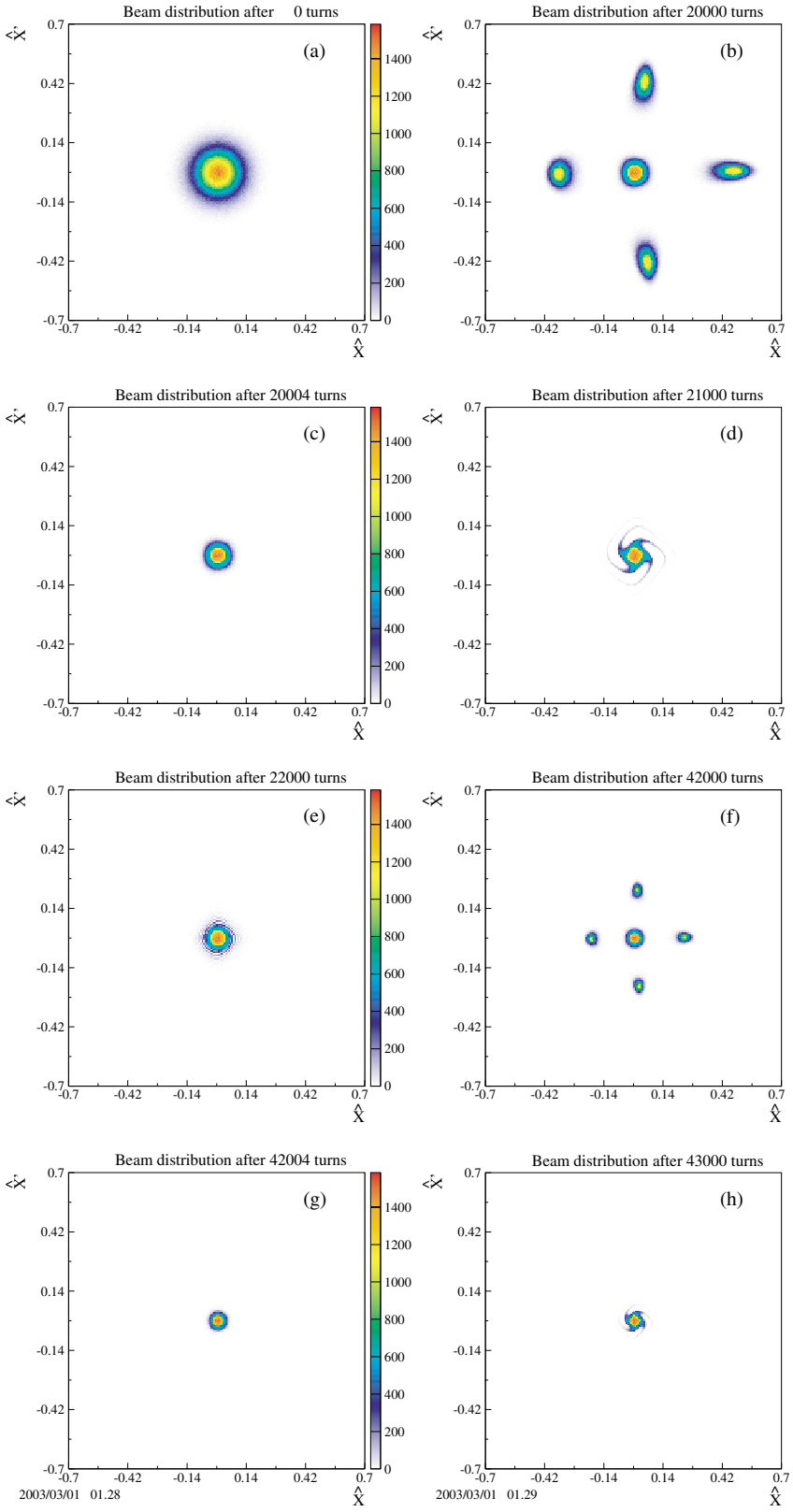

FIG. 12. (Color) Beam distribution during the multiple multiturn extraction for the fourth-order resonance (8.1×10^5 initial conditions). The initial distribution is a Gaussian centered on zero, with standard deviation $\sigma = 0.07$. The value of κ is changed according to the curve shown in Fig. 11.

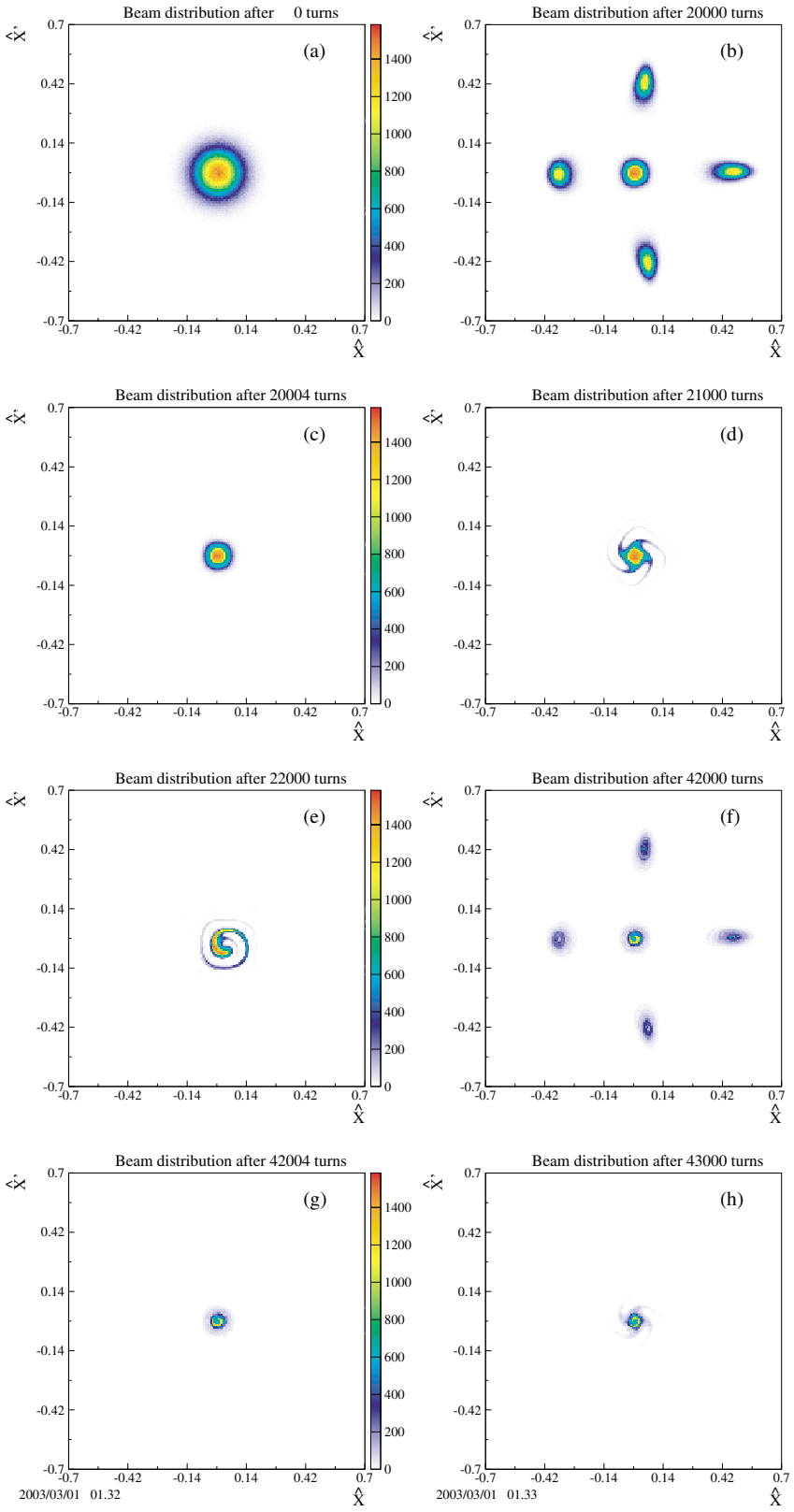

FIG. 13. (Color) Beam distribution during the multiple multiturn extraction for the fourth-order resonance (8.1×10^5 initial conditions). The initial distribution is a Gaussian centered on zero, with standard deviation $\sigma = 0.07$. $\kappa = -1.5$, but the beam size is increased by repeated kicks after each extraction.

of the magnetic field, and ℓ is the physical length of the magnetic element. In the following it will be assumed that $J_n = 0$ for $n \geq 2$.

It is customary to change coordinates from physical to Courant-Snyder ones [11]. This is obtained by means of the linear, symplectic transformation:

$$\begin{pmatrix} \hat{z} \\ \hat{z}' \end{pmatrix} = T_z^{-1} \begin{pmatrix} z \\ z' \end{pmatrix}, \qquad T_z = \begin{pmatrix} \sqrt{\beta_z} & 0 \\ -\frac{\alpha_z}{\sqrt{\beta_z}} & \frac{1}{\sqrt{\beta_z}} \end{pmatrix}, \tag{A5}$$

where z stands for x or y and the quantities α_z, β_z are the Twiss parameters [11] at the location of the nonlinear elements. The general 4D normalization matrix T is in block diagonal form,

$$T = \begin{pmatrix} T_x & 0 \\ 0 & T_y \end{pmatrix}. \tag{A6}$$

By taking into account that

$$\begin{aligned} R(\omega_x, \omega_y) &= T^{-1} M T, \\ R(\omega_x, \omega_y) &= \begin{pmatrix} R(\omega_x) & 0 \\ 0 & R(\omega_y) \end{pmatrix}, \end{aligned} \tag{A7}$$

with $R(\omega_z)$ a 2×2 rotation matrix,

$$R(\omega_z) = \begin{pmatrix} \cos\omega_z & \sin\omega_z \\ -\sin\omega_z & \cos\omega_z \end{pmatrix}, \qquad \omega_z = 2\pi\nu_z, \tag{A8}$$

the mapping (A1) reads in the new coordinates

$$\begin{pmatrix} \hat{x} \\ \hat{x}' \\ \hat{y} \\ \hat{y}' \end{pmatrix}_{n+1} = R(\omega_x, \omega_y) \begin{pmatrix} \hat{x} \\ \hat{x}' + \sqrt{\beta_x} f_x(\sqrt{\beta_x}\hat{x}, \sqrt{\beta_y}\hat{y}) \\ \hat{y} \\ \hat{y}' + \sqrt{\beta_y} f_y(\sqrt{\beta_x}\hat{x}, \sqrt{\beta_y}\hat{y}) \end{pmatrix}_n. \tag{A9}$$

The general expression for the nonlinear kicks in the new coordinates can be obtained by using expression (A3). In the computations presented in this paper only the first two terms, corresponding to the sextupolar and octupolar components, are taken into account:

$$n = m = 2 \begin{cases} \sqrt{\beta_x} f_x(\sqrt{\beta_x}\hat{x}, \sqrt{\beta_y}\hat{y}) = \frac{K_2}{2} \beta_x^{3/2} (\hat{x}^2 - \chi \hat{y}^2), \\ \sqrt{\beta_y} f_y(\sqrt{\beta_x}\hat{x}, \sqrt{\beta_y}\hat{y}) = -K_2 \beta_x^{3/2} \chi \hat{x}\hat{y}, \end{cases} \tag{A10}$$

$$n = m = 3 \begin{cases} f_x(\sqrt{\beta_x}\hat{x}, \sqrt{\beta_y}\hat{y}) = \frac{K_3}{6} \beta_x^2 (\hat{x}^3 - 3\chi \hat{x}\hat{y}^2), \\ f_y(\sqrt{\beta_x}\hat{x}, \sqrt{\beta_y}\hat{y}) = -\frac{K_3}{6} \beta_x^2 (\chi^2 \hat{y}^3 - 3\chi \hat{x}^2 \hat{y}), \end{cases} \tag{A11}$$

where χ is a dimensionless parameter given by $\chi = \beta_y/\beta_x$.

The next step consists of rescaling the Courant-Snyder coordinates to set the coefficient of the quadratic term in (A9) equal to 1. By means of a nonsymplectic transformation it is possible to define new dimensionless coordinates $(\hat{X}, \hat{X}', \hat{Y}, \hat{Y}') = \lambda(\hat{x}, \hat{x}', \hat{y}, \hat{y}')$ such that the one-turn map can be recast in the following form:

$$\begin{pmatrix} \hat{X} \\ \hat{X}' \\ \hat{Y} \\ \hat{Y}' \end{pmatrix}_{n+1} = R(\omega_x, \omega_y) \begin{pmatrix} \hat{X} \\ \hat{X}' + \lambda\sqrt{\beta_x} f_x(\sqrt{\beta_x}\frac{\hat{X}}{\lambda}, \sqrt{\beta_y}\frac{\hat{Y}}{\lambda}) \\ \hat{Y} \\ \hat{Y}' + \lambda\sqrt{\beta_y} f_y(\sqrt{\beta_x}\frac{\hat{X}}{\lambda}, \sqrt{\beta_y}\frac{\hat{Y}}{\lambda}). \end{pmatrix}_n, \tag{A12}$$

With the choice $\lambda = 1/2K_2 \beta_x^{3/2}$ one obtains the following expression for the nonlinear kicks in Eq. (A12):

$$n = m = 2 \begin{cases} \lambda\sqrt{\beta_x} f_x(\sqrt{\beta_x}\frac{\hat{X}}{\lambda}, \sqrt{\beta_y}\frac{\hat{Y}}{\lambda}) = \hat{X}^2 - \chi \hat{Y}^2, \\ \lambda\sqrt{\beta_y} f_y(\sqrt{\beta_x}\frac{\hat{X}}{\lambda}, \sqrt{\beta_y}\frac{\hat{Y}}{\lambda}) = -2\chi \hat{X}\hat{Y}, \end{cases} \tag{A13}$$

$$n = m = 3 \begin{cases} \lambda\sqrt{\beta_x} f_x(\sqrt{\beta_x}\frac{\hat{X}}{\lambda}, \sqrt{\beta_y}\frac{\hat{Y}}{\lambda}) = \kappa(\hat{X}^3 - 3\chi \hat{X}\hat{Y}^2), \\ \lambda\sqrt{\beta_y} f_y(\sqrt{\beta_x}\frac{\hat{X}}{\lambda}, \sqrt{\beta_y}\frac{\hat{Y}}{\lambda}) = -\kappa(\chi^2 \hat{Y}^3 - 3\chi \hat{X}^2 \hat{Y}), \end{cases} \tag{A14}$$

with

$$\kappa = \frac{2}{3} \frac{K_3}{K_2^2} \frac{1}{\beta_x}. \tag{A15}$$

The expression of higher-order multipoles in the final coordinates can be obtained easily by means of the following substitution:

$$\frac{K_n + iJ_n}{n!} \rightarrow \frac{2^{n-1}}{K_2^{n-1} \beta_x^{3(n-1)/2}} \frac{K_n + iJ_n}{n!}. \tag{A16}$$

APPENDIX B: FIXED POINTS

In this section some theorems concerning fixed points of a special class of 2D symplectic maps derived in Ref. [13] will be reported. They are based on results discussed in Refs. [14,15].

A symplectic map $\mathbf{F}$ of $\mathbb{R}^{2n}$ is called reversible if it is the product of two involutions, namely,

$$\mathbf{F} = \mathcal{I}_1 \circ \mathcal{I}_2 \quad \text{with} \quad \mathcal{I}_1^2 = \mathcal{I}_2^2 = I, \tag{B1}$$

where I is the identity matrix in $\mathbb{R}^{2n}$. Such a factorization imposes constraints on the existence and location of the fixed points and can be used to simplify the problem of their computation. A point $\mathbf{x}$ is called a fixed point of $\mathbf{F}$ if it satisfies the equation

$$\mathbf{F}(\mathbf{x}) = \mathbf{x}. \tag{B2}$$

Similarly, fixed points of order m, or m cycles, can be defined as the fixed points of the mth iterate of the map

$$\mathbf{F}^{\circ m}(\mathbf{x}) = \mathbf{x}, \quad \text{where } \mathbf{F}^{\circ m}(\mathbf{x}) = \underbrace{\mathbf{F}(\mathbf{F}(\mathbf{F}(\cdots \mathbf{F}}_{m \text{ times}}(\mathbf{x})\cdots))). \tag{B3}$$

One can prove that [13].

Theorem 1.—Given a symplectic map $\mathbf{F}$ of $\mathbb{R}^{2n}$ such that $\mathbf{F} = \mathcal{I}_1 \circ \mathcal{I}_2$ with $\mathcal{I}_1, \mathcal{I}_2$ two involutions, if $\mathbf{x}$ is a point of $\mathbb{R}^{2n}$ satisfying

$$\begin{cases} \mathcal{I}_1(\mathbf{x}) = \mathbf{x}, \\ \mathcal{I}_2(\mathbf{F}^{\circ m}(\mathbf{x})) = \mathbf{F}^{\circ m}(\mathbf{x}), \end{cases} \tag{B4}$$

then $\mathbf{F}^{\circ 2m+1}(\mathbf{x}) = \mathbf{x}$.

Similarly, if $\mathbf{x}$ is a solution of one of the two systems

$$\begin{cases} \mathcal{I}_1(\mathbf{x}) = \mathbf{x}, \\ \mathcal{I}_1(\mathbf{F}^{\circ m}(\mathbf{x})) = \mathbf{F}^{\circ m}(\mathbf{x}), \end{cases} \qquad \begin{cases} \mathcal{I}_2(\mathbf{x}) = \mathbf{x}, \\ \mathcal{I}_2(\mathbf{F}^{\circ m}(\mathbf{x})) = \mathbf{F}^{\circ m}(\mathbf{x}), \end{cases} \tag{B5}$$

then $\mathbf{F}^{\circ 2m}(\mathbf{x}) = \mathbf{x}$.

In the case of 2D one-turn maps of the form described in Appendix A, it is easy to show that they can be decomposed into two involutions, with $\mathcal{I}_1$ and $\mathcal{I}_2$ being a linear and a nonlinear transformation, respectively,

$$\mathcal{I}_1 = \begin{pmatrix} \cos\omega_x & -\sin\omega_x \\ -\sin\omega_x & -\cos\omega_x \end{pmatrix},$$
$$\mathcal{I}_2(x, x') = \begin{pmatrix} x \\ -x' - P_r(x) \end{pmatrix}, \tag{B6}$$

where $P_r(x)$ is a polynomial of order r representing the effect of the kicks due to the nonlinear elements. It is easily seen that $\mathcal{I}_1$ represents a reflection about the line $x' = -x \tan\omega_x/2$, the locus of fixed points of $\mathcal{I}_1$. Similarly, the locus of fixed points of $\mathcal{I}_2$ is given by curve $x' = -1/2P_r(x)$.

Under these hypotheses it is possible to prove that the following stronger results hold [13].

Theorem 2.—Let $\mathbf{F}$ be a planar symplectic map factorized into involutions $\mathcal{I}_1, \mathcal{I}_2$ of the form given in Eq. (B6). Then $\mathbf{x}$ is a fixed point of $\mathbf{F}$ iff it satisfies

$$\begin{cases} \mathcal{I}_1(\mathbf{x}) = \mathbf{x}, \\ \mathcal{I}_2(\mathbf{x}) = \mathbf{x}. \end{cases} \tag{B7}$$

The geometrical interpretation of this theorem is that the fixed points of period one are exactly the intersections of the loci of the fixed points of the two transformations $\mathcal{I}_1, \mathcal{I}_2$ into which the map $\mathbf{F}$ is decomposed.

A similar result holds for the fixed points of $\mathbf{F}^{\circ 2}$.

Theorem 3.—Let $\mathbf{F}$ be a planar symplectic map factorized into involutions $\mathcal{I}_1, \mathcal{I}_2$ of the form given in Eq. (B6). Then $\mathbf{x}$ is a fixed point of $\mathbf{F}^{\circ 2}$ iff it fulfils the following condition:

$$\begin{cases} \mathcal{I}_2(\mathbf{x}) = \mathbf{x}, \\ \mathcal{I}_2(\mathbf{F}(\mathbf{x})) = \mathbf{F}(\mathbf{x}). \end{cases} \tag{B8}$$

Condition (B8) means that if both the initial point $\mathbf{x}$ and its image under $\mathbf{F}$ belong to the locus of the fixed points of $\mathcal{I}_2$, then $\mathbf{x}$ is a fixed point of $\mathbf{F}^{\circ 2}$. However, the action of $\mathbf{F}$ on a fixed point of $\mathcal{I}_2$ is simply a reflection about the fixed line of $\mathcal{I}_1$. Therefore, provided trivial solutions, i.e., fixed points of $\mathbf{F}$ are disregarded, for a fixed point of period two to exist the locus of fixed points of $\mathcal{I}_2$ must contain at least one point together with its reflection about the fixed line of $\mathcal{I}_1$. It is easily seen that this can never be the case for maps of the form (2).

To overcome this difficulty the initial map has to be modified to break the symmetry and the factorization into the two involutions $\mathcal{I}_1$ and $\mathcal{I}_2$. This can be obtained by separating the two sources of nonlinearities, i.e., sextupole and octupole magnets, hence inserting a linear matrix between the two nonlinear kicks, as it is the case with the new map (3).

[1] C. Bovet, D. Fiander, L. Henny, A. Krusche, and G. Plass, in *Proceedings of the 1973 Particle Accelerator Conference*, edited by D.W. Dupen (IEEE, New York, 1973), p. 438.

[2] R. Cappi and M. Giovannozzi, CERN Report No. PS 2002-083 (AE), 2002 (unpublished).

[3] R. Bailey, J.-L. Baldy, A. Ball, P. Bonnal, M. Buhler-Broglin, C. Détraz, A. Ereditato, P.-E. Faugeras, A. Ferrari, G. Fortuna, A. L. Grant, A.-M. Guglielmi, A. Hilaire, K. Hübner, M. Jonker, K. H. Kissler, L.-A. López-Hernandez, J.-M. Maugain, P. Migliozzi, V. Palladino, F. Pietropaolo, J.-P. Revol, P. R. Sala, C. Sanelli, G. R. Stevenson, N. Vassilopoulos, H. H. Vincke, E. Weisse, and M. Wilhemsson, CERN Report No. 98-02, 1998, edited by K. Elsener (unpublished).

[4] K. Cornelis, J.-P. Delahaye, R. Garoby, H. Haseroth, K. Hübner, T. Linnecar, S. Myers, K. Schindl, and C. Wyss, CERN Report No. CERN-PS 2001-041 (AE), 2001, edited by R. Cappi (unpublished).

[5] R. Cappi and M. Giovannozzi, Phys. Rev. Lett. **88**, 104801 (2002).

[6] R. Cappi and M. Giovannozzi, in *Proceedings of the Eighth European Particle Accelerator Conference, Paris, 2002*, edited by J. Poole and C. Petit-Jean-Genaz (IOP, London, 2002), p. 1250.

[7] A. J. Lichtemberg and M. A. Lieberman, *Regular and Chaotic Dynamics* (Springer-Verlag, New York, 1992).

[8] R. Cappi, M. Giovannozzi, M. Martini, E. Métral, G. Métral, A.-S. Müller, and R. Steerenberg, in *Proceedings of the 2003 Particle Accelerator Conference*, edited by J. Chew, P. Lucas, and S. Webbers (IEEE, Piscataway, NJ, 2003), p. 388; CERN Report No. CERN-AB-2003-015, 2003 (unpublished).

[9] A. Bazzani, G. Servizi, E. Todesco, and G. Turchetti, CERN Report No. 94-02, 1994 (unpublished).

[10] M. Hénon, Q. Appl. Math. **27**, 291 (1969).
[11] E. Courant and H. Snyder, Ann. Phys. (Paris) **3**, 1 (1958).
[12] D. Edwards and L. Teng, IEEE Trans. Nucl. Sci. **20**, 885 (1973).
[13] M. Giovannozzi, Phys. Rev. E **53**, 6403 (1996).
[14] R. De Vogelaere, in *Contributions to the Theory of Non-Linear Oscillations*, edited by S. Lefschetz (Princeton University Press, Princeton, 1958), Vol. IV, p. 53.
[15] J. M. Finn, Ph.D. thesis, University of Maryland, 1974.
[16] A.W. Chao and M. Month, Nucl. Instrum. Methods **121**, 129 (1974).